Synthesis and Assembly of Designer Styrenic Diblock Polyelectrolytes

Jeffrey M. Ting,[†,‡] Hao Wu,[†] Abraham Herzog-Arbeitman,[§] Samanvaya Srivastava,[⊥] and Matthew V. Tirrell[*,†,‡]

† Institute for Molecular Engineering, University of Chicago, Chicago, Illinois 60637, United States. ‡ Argonne National Laboratory, Lemont, Illinois 60439, United States. § Department of Chemistry, University of Chicago, Chicago, Illinois 60637, United States. ⊥ Department of Chemical and Biomolecular Engineering, University of California, Los Angeles, Los Angeles, California 90095, United States.

KEYWORDS: RAFT polymerization, polyelectrolyte, polyelectrolyte complexation, micelles.

ABSTRACT: Harnessing new molecular design principles toward functional applications of ion-containing macromolecules relies on diversifying experimental datasets of well-understood materials. Here, we report a simple, tunable framework for preparing styrenic polyelectrolytes, using aqueous reversible addition-fragmentation chain transfer (RAFT) polymerization in a parallel synthesis approach. A series of diblock polycations and polyanions were RAFT chain-extended from polyethylene oxide (PEO) using (vinylbenzyl)trimethylammonium chloride (PEO-*b*-PVBTMA) and sodium 4-styrenesulfonate (PEO-*b*-PSS), with varying neutral PEO block lengths, charged styrenic block lengths, and RAFT end-group identity. The materials characterization and kinetics study of chain growth exhibited control of the molar mass distribution for both systems. These block polyelectrolytes were also demonstrated to form polyelectrolyte complex (PEC) driven self-assemblies. We present two simple outcomes of micellization to show the importance of polymer selection from a broadened pool of polyelectrolyte candidates: (*i*) uniform PEC-core micelles comprising PEO-*b*-PVBTMA and poly(acrylic acid), and (*ii*) PEC nanoaggregates comprising PEO-*b*-PVBTMA and PEO-*b*-PSS. The materials characteristics of these charged assemblies were investigated with dynamic light scattering, small angle X-ray scattering, and cryogenic-transmission electron microscopy imaging. This model synthetic platform offers a straightforward path to expand the design space of conventional polyelectrolytes into gram-scale block polymer structures, which can ultimately enable the development of more sophisticated ionic materials into technology.

The U.S. Materials Genome Initiative (MGI) is a national movement launched over half a decade ago in 2011, built on the core mission of accelerating the discovery-to-deployment cycle of new materials innovation and end-use technologies.[1] This program provides a framework for *materials by design* – new classes of hard and soft matter developed by integrating theory, computation, and experiment together across universities, industries, and national laboratories.[2,3] Recent MGI-supported works span a wide breadth of applications, from organic solar cells[4] and low-dimension nanoelectric heterojunction[5] to self-assembled DNA-nanoparticle crystals.[6] In these materials platforms, a recurring theme is the establishment of fundamental knowledge for predicting functionality and complexity across multiple hierarchical length and time scales. For polymeric materials, central to this endeavor is the advancement of tunable materials platforms that can build new relationships between molecular-level structure and macroscopic properties for challenging materials systems, such as soft materials that interface with biological environments.

Polyelectrolyte complexes (PECs) represent a prominent class of such biorelevant materials that can greatly benefit from this MGI approach. In particular, self-assembled micelles containing hydrated PEC cores surrounded by outer hydrophilic coronas are useful delivery vehicles for emerging technologies, such as the controlled delivery of drug or genetic payloads, regenerative medicine, agricultural innovations, and water purification strategies.[7-10] Engineering these oppositely charged polymeric assemblies in aqueous environments to exhibit desirable performance and required stability, however, remains extremely difficult.[11] Compared to their uncharged, amphiphilic block polymer counterparts, PEC micelles are subject to additional non-covalent intermolecular interactions, e.g., electrostatic associations, hydrogen bonding, multivalency in ion binding, π-π stacking interactions, chirality, sequencing, and solvent buffering capacity.[12-15] The confluence of these interactions affects not only particle size but also material properties, such as whether PEC domains form liquid-like coacervates or solid-like precipitates. Numerous theories on polyelectrolyte coacervation exist in the form of models[16] and simulations[17] based on commercially-available polyelectrolyte systems, but to realize more universal theories, synthetic platforms with programmable molecular attributes that can finely probe discrete non-covalent interactions are needed.

To this end, we devised a straightforward approach for the rational design of modular polycation and polyanion block polymers. Reversible-deactivation radical polymerization techniques offer the ability to target precise molar masses with narrow dispersity in chain-length distribution. Reversible addition-fragmentation chain transfer (RAFT) polymerization is distinguished for being viable for many vinyl monomer families,[18] tolerant in aqueous settings,[19-20] amenable to high-throughput schemes[21,22] or under flow,[23] and versatile in chain transfer agent (CTA) extension to higher-order blocks as well as bioconjugation with targeting moieties or theranostic mark-

ers.[24,25] RAFT CTAs are often commercially available[26] or readily synthesized[27] for nearly any given vinyl monomer type. In a recent perspective, Perrier highlighted the versatility of RAFT polymerization for experts and newcomers alike as an enabling tool to prepare sophisticated materials across scientific disciplines.[28] Thus, this technique can be readily adapted to prepare block polyelectrolytes with prescribed molecular attributes to address the effects of neutral-to-charged block lengths, end groups, and ionic strength on the complex assembly structure and function.

We apply this approach here to the synthesis of diblock polyelectrolytes from two poly(ethylene oxide) (PEO) macromolecular CTAs (macro-CTAs) with degree of polymerizations (DPs) of 112 and 225. We demonstrate the synthesis of two water-soluble styrenic systems that are pertinent to biomedical and energy applications: poly((vinylbenzyl)trimethylammonium chloride) (PVBTMA) and poly(sodium 4-vinylbenzenesulfonate) (or synonymously, polystyrene sulfonate PSS) as the polycation and polyanion blocks, respectively. PVBTMA homopolymers have been employed in examples from polyplexes for gene therapy[29] to anion exchange membrane fuel cells.[30] Likewise, PSS homopolymers have been incorporated into numerous materials platforms that exploit its high ionic conductivity, from heparin mimic for protein stabilization[31] to unipolar ion-conducting materials for thermoelectrics.[32] Scheme 1 shows the parallel synthesis of these polyelectrolyte pairs, using thermal initiator VA-044 (with a macro-CTA to VA-044 molar ratio of 10:1) at 50 °C in deoxygenated acetate buffer solvent (pH 5.2) to minimize chain end hydrolysis/aminolysis.[33]

Scheme 1. Synthesis of Diblock Polyelectrolytes with Aqueous RAFT Polymerization. [a]

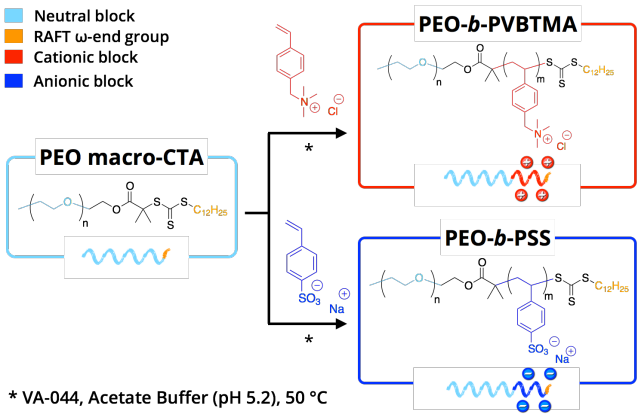

[a] RAFT polymerizations were conducted at a PEO macro-CTA to water-soluble azo initiator VA-044 molar equivalence of 10 to 1.

While these individual building blocks are of considerable interest, limited examples of constructing them into block architectures with controlled RAFT polymerization exist. In 1998, Rizzardo, Moad, San Thang, and coworkers at CSIRO reported the first successful aqueous RAFT polymerization to prepare a homopolymer of PSS.[34] Later, McCormick and coworkers prepared aqueous RAFT polymerizations of PSS-*b*-poly(sodium 4-vinylbenzoate) and PVBTMA-*b*-poly(*N*,*N*-dimethylvinylbenzylamine),[35] followed by examples of potential uses of modifying gold film surfaces.[36] Two other notable examples of RAFT-mediated block polymers have been reported. First, Haladjova et al. prepared poly[oligo(ethylene glycol) methacrylate]-*b*-PVBTMA as gene delivery vectors,[29] although the molecular weight distributions of the polymers were not reported. Second, PSS-*b*-PEO-*b*-PSS has been synthesized from a bifunctional PEO macro-CTA.[37,38] Collectively, these works motivated us to outline a single, systematic protocol for preparing sets of PEO-*b*-PVBTMA and PEO-*b*-PSS diblocks as a model synthetic platform for future polyelectrolyte studies.

For the nomenclature, subscripts next to the polymer block denote the DP. As an initial set of diblock polyelectrolytes, we used the following commercially-available PEO macro-CTAs: PEO_{112} and PEO_{225} methyl ether (2-methyl-2-propionic acid dodecyl trithiocarbonate) (PEO_{112}-$C_{12}H_{25}$ and PEO_{225}-$C_{12}H_{25}$), and PEO_{225} 4-cyano-4-(phenylcarbonothioylthio)pentanoate (PEO_{225}-Sty). These PEO macro-CTAs were chain extended with PVBTMA or PSS blocks so that the charged block length was either half the PEO block length (e.g., PEO_{112}-*b*-$PVBTMA_{50}$-$C_{12}H_{25}$) or approximately equal to the PEO block length (e.g., PEO_{112}-*b*-$PVBTMA_{100}$-$C_{12}H_{25}$). In the spirit of emphasizing materials discovery in the MGI, a parallel synthesizer was employed to enhance the pace of laboratory polymers preparation. This carousel instrument allowed twelve 20 mL reactor tubes to be simultaneously stirred, deoxygenated, heated, and visually monitored per experimental run on a single hotplate; ~3 g of each block polyelectrolyte was targeted per reactor. We anticipate that instrumentation like this can assist in the expansion of materials development and the establishment of structure-property relationships.

All reactions were conducted for 21 h and purified by dialysis. Table 1 summarizes the characterization of the polyelectrolytes, detailing the DP of each block, number-average molecular weight (M_n) of the polymer, dispersity ($Đ$), and degradation temperature (T_d) as identified using thermogravimetric analysis (TGA). By ^{1}H NMR spectroscopy, the total monomer conversion of all systems exhibited near-quantitative conversion after 21 h. Because of the ionic and hydrophobic nature of the styrenic block, the aqueous size-exclusion chromatography (SEC) mobile phase was optimized with salt and weak organic solvents to minimize secondary effects (i.e., column interactions shown in Fig. S-9). The absolute M_n was evaluated with SEC with multi-angle light scattering (SEC-MALS) and ^{1}H NMR spectroscopy, which exhibited relatively good experimental agreement. Low $Đ$ values indicate good control of the aqueous RAFT polymerizations using the carousel apparatus. However, we note that the SEC-MALS data of the as-received PEO_{225}-Sty exhibited a large molecular-weight shoulder (hypothesized to be coupled PEO upon macro-CTA synthesis, shown in Fig. S-2), which resulted in higher M_n diblocks due to the effectively lower macro-CTA to monomer ratio. By thermogravimetric analysis, two thermal degradations signifying each distinct block across all prepared systems were observed (Fig. S-13). The relatively high T_d values allow these materials to be useful in various high-temperature polymer processing applications.

Table 1. Polymer Characterization of Prepared Diblock Polyelectrolytes.

System	DP_{PEO} [a]	$DP_{charged}$ [a]	ω-end group [b]	Conv. [c] (%)	$M_{n,SEC}$ [d] (kg/mol)	$M_{n,NMR}$ [e] (kg/mol)	$Đ$ [f]	T_d [g] (°C)
PEO-*b*-PVBTMA	112	53	$–C_{12}H_{25}$	>99	18.3	16.2	1.12	199, 378
	112	105	$–C_{12}H_{25}$	>99	30.9	27.2	1.08	209, 389
	225	100	$–C_{12}H_{25}$	>99	29.1	31.2	1.17	212, 366
	225	80	–Sty	N/A	36.0	28.5	1.09	209, 369
	225	194	$–C_{12}H_{25}$	>99	47.7	51.6	1.11	236, 372
	225	198	–Sty	N/A	65.5	52.0	1.20	278, 379
PEO-*b*-PSS	112	41	$–C_{12}H_{25}$	>99	19.8	13.5	1.34	269, 460
	112	86	$–C_{12}H_{25}$	>99	31.3	22.7	1.22	271, 461
	225	80	$–C_{12}H_{25}$	85	34.6	26.6	1.23	269, 464
	225	70	–Sty	N/A	39.5	24.5	1.27	272, 465
	225	162	$–C_{12}H_{25}$	N/A	- [h]	43.4	- [h]	277, 465
	225	166	–Sty	N/A	- [h]	44.3	- [h]	276, 467

[a] Degree of polymerization for the PEO (reported) and charged blocks (by ^{1}H NMR spectroscopy in D_2O). [b] RAFT ω-end group: $–C_{12}H_{25}$ denotes (2-methyl-2-propionic acid dodecyl trithiocarbonate), and –Sty denotes 4-cyano-4-(phenylcarbonothioylthio)pentanoate. [c] Total monomer conversion, after 12 h at 50 °C via ^{1}H NMR spectroscopy of the crude aliquot in D_2O. N/A = no NMR data available. [d] Experimentally-measured M_n, determined by SEC-MALS at 35 °C. For PEO-*b*-PVBTMA, acetonitrile/water (40/60, %, *v*/*v*) with 0.1% trifluoroacetic acid was used; for PEO-*b*-PSS, methanol, acetonitrile, and 0.1 M $NaNO_3$ + 0.02 wt % NaN_3 water (15/15/70, %, *v*/*v*/*v*) was used. We note that since NaN_3 is known to cleave RAFT thiol-end groups,[39] samples were dissolved and immediately run. d*n*/dc values in each respective mixture are in Table S-2. [e] Experimentally-measured M_n by ^{1}H NMR spectroscopy in D_2O using M_n = sum of monomer molar mass × measured molar composition in polymer × degree of polymerization, assuming one RAFT agent per chain and 100% conversion. [f] Dispersity ($Đ$) = M_w / M_n. [g] Degradation temperature (T_d) by thermogravimetric analysis. [h] Not available due to SEC column interactions.

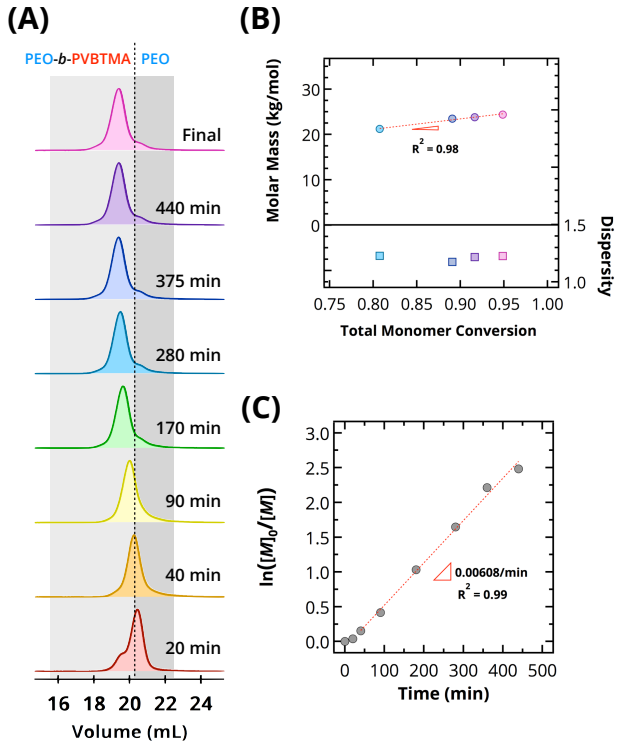

Figure 1. Kinetics of PEO_{225}-*b*-$PVBTMA_{100}$–$C_{12}H_{25}$: (A) the evolution of normalized SEC-MALS chromatograms over time (RI detector, shifted vertically for clarity), (B) a summary of molar mass (by ^{1}H NMR spectroscopy) and dispersity (by SEC-MALS) versus total monomer conversion, and (C) the pseudo-first-order kinetics plot, fitted to the equation $\ln([M]_0/[M]) = k_p^{app}[I]_0 t$ (the dashed red lines indicate a linear regression).

To demonstrate the control of the aqueous RAFT reactions, we examined the kinetics of PEO_{225}-*b*-$PVBTMA_{100}$-$C_{12}H_{25}$ and PEO_{225}-*b*-PSS_{100}-$C_{12}H_{25}$. The progress of each polymerization was monitored over time by ^{1}H NMR spectroscopy to determine the total monomer conversion (Fig. S-16); crude aliquots were collected and purified by dialysis for SEC-MALS analysis. Fig. 1 shows the PEO_{225}-*b*-$PVBTMA_{100}$-$C_{12}H_{25}$ reaction. From the SEC chromatograms overlay, the PEO macromolecular chain extension reaction can be directly observed: the molecular weight distribution of the PEO macro-CTA (initially centered at ~ 20.4 mL) decreased in signal intensity and shifts to lower elution volume over time, indicating the chain growth of the charged block (Fig. 1-A). Furthermore, the linear increase in M_n as a function of total monomer conversion with low $Đ$ suggests that the reaction was well controlled (Fig. 1-B). The same general trend was observed for the PEO_{225}-*b*-PSS_{112}-$C_{12}H_{25}$ system (Fig. S-17).

In addition, we determined the apparent rate constant of propagation (k_p^{app}). Assuming that the rate of polymer formation (i.e., rate of propagation R_p) is equal to the rate at which monomers are consumed at a quasi-steady state, Equation 1 can be derived,[40] which assesses the living character of a polymerization in the absence of termination:

$$\ln\left(\frac{[M]_0}{[M]}\right) = k_p^{app}[I]_0 t \qquad [1]$$

Here, $[M]_0/[M]$ is the ratio of the initial monomer concentration to the monomer concentration at time t, and $[I]_0$ is the initial initiator concentration. Pseudo-first-order kinetics were observed, as is evident from a linear growth of $\ln([M]_0/[M])$ over time for both PEO_{225}-*b*-$PVBTMA_{100}$–$C_{12}H_{25}$ (Fig. 1-C; R^2 = 0.99) and PEO_{225}-*b*-PSS_{100}–$C_{12}H_{25}$ (Fig. S-17; R^2 = 0.98). These trends confirm excellent control of the reaction under

these experimental conditions. We note that the linear fits have a nonzero intercept due to the induction time for the RAFT initialization/reinitiation steps. The k_p^{app} values were similar, calculated from the slopes to be 0.10 and 0.11 $M^{-1}s^{-1}$ for PEO_{225}-*b*-$PVBTMA_{112}$–$C_{12}H_{25}$ and PEO_{225}-*b*-PSS_{112}–$C_{12}H_{25}$, respectively.

The representative set of new materials prepared above can be readily combined with model polymers to systematically address open questions in how chemistry affects charge-driven self-assembly. The physical preparation process is known to affect the formation of uncharged amphiphilic micelles, due to the block lengths, the nature of the hydrophobic constituent block, cosolvent effects, and other secondary interactions.[41-43] It is difficult to predict *a priori* the nature and properties of an ionic complex based on a desired polycation and polyanion. The Schlenoff laboratory has comprehensively examined the ion-pairing strengths of positively- and negatively-charged homopolymers with salt,[44-46] leading to an increased general understanding of the bulk complexation process. Our group has focused on providing a quantitative description of the phase behavior of bulk homopolyelectrolytes,[47] as well as employing a PEO/poly(allyl glycidyl ether) platform towards gel network design.[48,49] However, to the extent of our knowledge, observations from bulk complexation have not been successfully extended to the design self-assembled structures. We believe that this RAFT materials platform can enable analogous studies by offering a straightforward avenue to construct well-studied polyelectrolytes in the complexation literature into compartmentalized, PEC-core assemblies.

To demonstrate this idea, we investigated the complex-core assemblies of PEO_{225}-*b*-$PVBTMA_{100}$–$C_{12}H_{25}$ with (1) poly(acrylic acid sodium salt) (PAA_{158}, a conventional weak polyanion, DP = 158) or (2) PEO_{225}-*b*-PSS_{80}–$C_{12}H_{25}$ (a strong polyanion). PECs of the PVBTMA and PAA homopolyelectrolytes have reportedly formed liquid-like coacervates with high water content, while pairing PVBTMA with PSS resulted in more kinetically-trapped structures.[45] A combination of cryogenic-transmission electron microscopy (cryo-TEM), dynamic light scattering (DLS), and small angle X-ray scattering (SAXS) was employed to fully characterize the PEC assemblies in deionized water. Because of the hydrophobic end-groups, the micellization of individual systems was first checked. All synthesized polyelectrolytes exhibited a critical micelle concentration above 10 mg/mL (Figs. S-14 and S-15), well above the 1 mg/mL dilute concentrations for the micelle studies involving charge-driven assemblies.

In the PEO_{225}-*b*-$PVBTMA_{100}$–$C_{12}H_{25}$/PAA_{158} system, cryo-TEM imaging illustrated the sphere-like morphology of the micelle cores (Fig. 2-A), with a mean particle diameter of 25 ± 7 nm (95% CI = 24.2, 26.0) and an interquartile range of 9.26 nm. For visualizing native soft matter, little contrast is expected between the hydrated PEO corona and the surrounding vitrified water. Complementary scattering studies to study the PEC corona confirmed this hypothesis. By multi-angle DLS, the micelles exhibited a unimodal size distribution with an apparent mean hydrodynamic radius (R_h) of 30 nm that did not evolve over time (Fig. 2-B). Furthermore, the observed linear angular dependence of the relaxation rate Γ as a function of the squared scattering wave vector q^2 from θ = 40-140° is a characteristic signature of the diffusive mode of spherical scatters (Figs. S-20-S-22). Finally, the intensity profile in the SAXS pattern exhibits a clear plateau up to q ~0.02 nm^{-1}, followed by a $I(q) \sim q^{-4}$ dependency, which indicates that the micelle core has a spherical geometry with an approximate diameter of 28 nm when fitted with a polydisperse core-shell model (see the Supporting Information for the mathematical details). This is in excellent agreement with the particles observed through cryo-imaging.

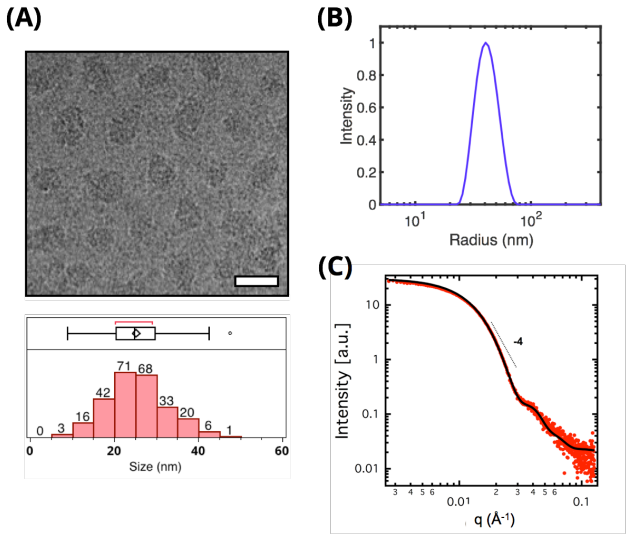

Figure 2. Solution assemblies of PEO_{225}-*b*-$PVBTMA_{100}$–$C_{12}H_{25}$/PAA_{158} at 1 mg/mL, characterized by (A) representative cryo-TEM imaging to visualize particles (scale bar represents 40 nm; modified box plot details in Fig. S-18), (B) DLS to determine the apparent hydrodynamic radius distribution (analyzed with REPES[44] at θ = 90°), and (C) SAXS to quantify morphology/size (red circles denote experimental data; black line represents a fitting to a polydisperse core-shell model).

In contrast, when PEO_{225}-*b*-$PVBTMA_{100}$–$C_{12}H_{25}$ was combined with PEO_{225}-*b*-PSS_{100}–$C_{12}H_{25}$, large, interconnected nanoaggregates with high particle polydispersity were observed from cryo-TEM imaging (Fig. 3-A). DLS analysis revealed a broad distribution of large structures that persisted for several weeks (Fig. S-23). A power-law slope of –1.6 in the *q*-range of $0.003 < q < 0.2$ $Å^{-1}$ suggested the existence of swollen coil-like structures[51] (Fig. 3-B). It is reasonable to infer that these aggregates are kinetically–trapped electrostatic assemblies. For uncharged amphiphilic diblock polymer systems, Lund and coworkers have demonstrated that micelle formation is subject to constant inter-micellar chain exchange.[52] The incomplete PEC micellization to uniform nanostructures may be attributed to the strong ionic nature of the PVBTMA and PSS blocks, whose ion–pairing is known to associate strongly,[45] thereby hindering polymer chains in electrostatic assemblies to escape and equilibrate over time. Nevertheless, these model materials can be used to explore the formation pathways and processing effects between kinetic and thermodynamic products, which has recently been of interest to the advancement of micelleplex delivery vehicles.[53-55] Detailed studies on the kinetics of formation and chain exchange in these PEC micelles are ongoing, and a following report is underway.

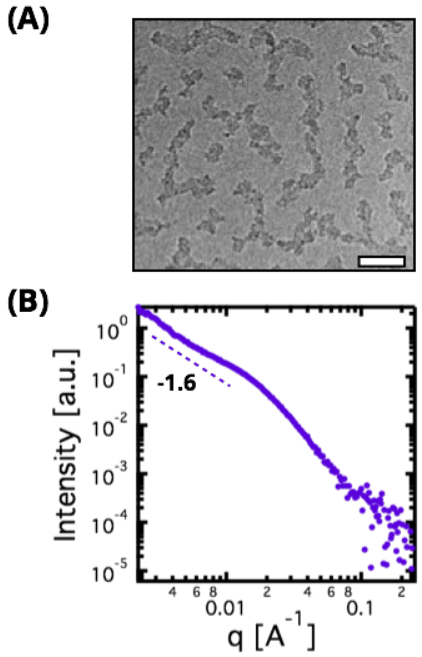

Figure 3. Solution assemblies of PEO_{225}-*b*-$PVBTMA_{100}$–$C_{12}H_{25}$ / PEO_{225}-*b*-PSS_{100}–$C_{12}H_{25}$ at 1 mg/mL, characterized by (A) cryo-TEM imaging to visualize particles (scale bar represents 40 nm) and (B) SAXS to quantify morphology and size.

Altogether, performing controlled aqueous RAFT polymerization of ionic monomers in a parallel reactor system is promising toward broadening the materials portfolio of designer PECs. The ease and versatility afforded by combining synthetic ingredients in a systematic manner enables molecular weight and chemical state spaces to be directly accessed, with additional opportunities to compare chain architecture effects. We are currently extending this synthesis capability to other monomer families (i.e., meth(acrylates), meth(acrylamides), etc.) in diblock and triblock arrangements. In this manner, rational combinations of strong and weak block polyelectrolytes can elucidate the consequences of chemical structure on resultant properties in PECs. Such design relationships can ultimately enhance the development of emerging applications at the materials science–biology interface that rely on charge complexation.

ASSOCIATED CONTENT

Supporting Information. The Supporting Information is available free of charge at the ACS Publications website (http://pubs.acs.org). Materials and Methods, Experimental Synthesis Details, Experimental Kinetics Details, Experimental Complex Assemblies Details, and Author Roles/Responsibilities (PDF).

AUTHOR INFORMATION

Corresponding Author

*E-mail: mtirrell@uchicago.edu (M.V.T.)

Author Contributions

The manuscript was written through contributions of all authors. All authors have given approval to the final version of the manuscript.

Notes

The authors declare no competing financial interests.

ACKNOWLEDGMENT

The authors gratefully thank Tera Lavoie, PhD in the Advanced Electron Microscopy Facility at the University of Chicago for her expertise and contributions to the cryo-imaging. The authors also acknowledge Xiaobing Zuo, PhD at the Advanced Photon Source in Argonne National Laboratory and Thomas Weiss, PhD at the Stanford Synchrotron Radiation Lightsource in SLAC National Accelerator Laboratory for their assistance in scattering experiments. This work was financially supported by the U.S. Department of Commerce, National Institute of Standards and Technology (NIST) through the Center for Hierarchical Materials Design (CHiMaD) under financial assistant award 70NANB14H012. J.M.T. acknowledges support from the NIST-CHiMaD Postdoctoral Fellowship. Parts of this work were carried out at the Soft Matter Characterization Facility of the University of Chicago. The use of the Advanced Photon Source, a U.S. Department of Energy (DOE) Office of Science User Facility operated for the DOE Office of Science by Argonne National Laboratory, was supported under Contract No. DE-AC02-06CH11357. Use of the Stanford Synchrotron Radiation Lightsource, SLAC National Accelerator Laboratory, is supported by the U.S. Department of Energy, Office of Science, Office of Basic Energy Sciences under Contract No. DE-AC02-76SF00515. The SSRL Structural Molecular Biology Program is supported by the DOE Office of Biological and Environmental Research, and by the National Institutes of Health, National Institute of General Medical Sciences (including P41GM103393). The contents of this publication are solely the responsibility of the authors and do not necessarily represent the official views of NIGMS or NIH.

REFERENCES

(1) Materials Genome Initiative. https://www.mgi.gov/ (accessed on May 4, 2018).

(2) White, A. The Materials Genome Initiative: One Year on. *MRS Bull.* **2012**, *37*, 715.

(3) de Pablo, J. J.; Jones, B.; Kovacs, C. L.; Ozolins, V.; Ramirez, A. P. The Materials Genome Initiative, the Interplay of Experiment, Theory and Computation. *Curr. Opin. Solid State Mater. Sci.* **2014**, *18*, 99.

(4) Zhao, D.; Wu, Q.; Cai, Z.; Zheng, T.; Chen, W.; Lu, J.; Yu, L. Electron Acceptors Based on A-Substituted Perylene Diimide (PDI) for Organic Solar Cells. *Chem. Mater.* **2016**, *28*, 1139.

(5) Jariwala, D.; Sangwan, V. K.; Seo, J.-W. T.; Xu, W.; Smith, J.; Kim, C. H.; Lauhon, L. J.; Marks, T. J.; Hersam, M. C. Large-Area, Low-Voltage, Antiambipolar Heterojunctions From Solution-Processed Semiconductors. *Nano Lett.* **2015**, *15*, 416.

(6) Lequieu, J.; Córdoba, A.; Hinckley, D.; de Pablo, J. J. Mechanical Response of DNA–Nanoparticle Crystals to Controlled Deformation. *ACS Cent. Sci.* **2016**, *2*, 614.

(7) Voets, I. K.; de Keizer, A.; Stuart, M. A. C. Advances in Colloid and Interface Science. *Adv. Colloid Interface Sci.* **2009**, *147-148*, 300.

(8) Freyer, J. L.; Brucks, S. D.; Campos, L. M. Fully Charged: Maximizing the Potential of Cationic Polyelectrolytes in Applications Ranging From Membranes to Gene Delivery Through Rational Design. *J. Polym. Sci. A Polym. Chem.* **2017**, *55*, 3167.

(9) Cummings, C. S.; Obermeyer, A. C. Phase Separation Behavior of Supercharged Proteins and Polyelectrolytes. *Biochemistry* **2017**, *57*, 314.

(10) Acar, H.; Ting, J. M.; Srivastava, S.; LaBelle, J. L.; Tirrell, M. V. Molecular Engineering Solutions for Therapeutic Peptide Delivery. *Chem. Soc. Rev.* **2017**, *46*, 6553.

(11) Muthukumar, M. 50th Anniversary Perspective: a Perspective on Polyelectrolyte Solutions. *Macromolecules* **2017**, *50*, 9528.

(12) Jackson, N. E.; Brettmann, B. K.; Vishwanath, V.; Tirrell, M.; de Pablo, J. J. Comparing Solvophobic and Multivalent Induced Collapse in Polyelectrolyte Brushes. *ACS Macro Lett.* **2017**, *6*, 155.

(13) Perry, S. L.; Leon, L.; Hoffmann, K. Q.; Kade, M. J.; Priftis, D.; Black, K. A.; Wong, D.; Klein, R. A.; Pierce, C. F.; Margossian, K. O.; et al. Chirality-Selected Phase Behaviour in Ionic Polypeptide Complexes. *Nat. Commun.* **2015**, *6*, 6052.

(14) Chang, L.-W.; Lytle, T. K.; Radhakrishna, M.; Madinya, J. J.; Vélez, J.; Sing, C. E.; Perry, S. L. Sequence and Entropy-Based Control of Complex Coacervates. *Nat. Commun.* **2017**, *8*, 213.

(15) Fu, J.; Schlenoff, J. B. Driving Forces for Oppositely Charged Polyion Association in Aqueous Solutions: Enthalpic, Entropic, but Not Electrostatic. *J. Am. Chem. Soc.* **2016**, *138*, 980.

(16) Srivastava, S.; Tirrell, M. V. *Advances in Chemical Physics*; John Wiley & Sons, Inc.: Hoboken, NJ, USA, 2016; Vol. 161, pp 499–544.

(17) Lytle, T. K.; Sing, C. E. Tuning Chain Interaction Entropy in Complex Coacervation Using Polymer Stiffness, Architecture, and Salt Valency. *Mol. Syst. Des. Eng.* **2018**, *3*, 183.

(18) Hill, M. R.; Carmean, R. N.; Sumerlin, B. S. Expanding the Scope of RAFT Polymerization: Recent Advances and New Horizons. *Macromolecules* **2015**, *48*, 5459.

(19) Lowe, A. B.; McCormick, C. L. Reversible Addition–Fragmentation Chain Transfer (RAFT) Radical Polymerization and the Synthesis of Water-Soluble (Co)Polymers Under Homogeneous Conditions in Organic and Aqueous Media. *Prog. Polym. Sci.* **2007**, *32*, 283.

(20) Schneiderman, D. K.; Ting, J. M.; Purchel, A. A.; Miranda, R.; Tirrell, M. V.; Reineke, T. M.; Rowan, S. J. "Open-to-Air RAFT Polymerization in Complex Solvents: From Whisky to Fermentation Broth" *ACS Macro Lett.* **2018**, *7*, 406.

(21) Ting, J. M.; Tale, S.; Purchel, A. A.; Jones, S. D.; Widanapathirana, L.; Tolstyka, Z. P.; Guo, L.; Guillaudeu, S. J.; Bates, F. S.; Reineke, T. M. High-Throughput Excipient Discovery Enables Oral Delivery of Poorly Soluble Pharmaceuticals. *ACS Cent. Sci.* **2016**, *2*, 748.

(22) Wu, H.; Yang, L.; Tao, L. Polymer Synthesis by Mimicking Nature's Strategy: the Combination of Ultra-Fast RAFT and the Biginelli Reaction. *Polym. Chem.* **2017**, *8*, 5679.

(23) Diehl, C.; Laurino, P.; Azzouz, N.; Seeberger, P. H. Accelerated Continuous Flow RAFT Polymerization. *Macromolecules* **2010**, *43*, 10311.

(24) Willcock, H.; O'Reilly, R. K. End Group Removal and Modification of RAFT Polymers. *Polym. Chem.* **2010**, *1*, 149.

(25) Abel, B. A.; McCormick, C. L. "One-Pot" Aminolysis/Thiol–Maleimide End-Group Functionalization of RAFT Polymers: Identifying and Preventing Michael Addition Side Reactions. *Macromolecules* **2016**, *49*, 6193.

(26) Moad, G.; Chiefari, J. RAFT: Choosing the Right Agent to Achieve Controlled Polymerization. https://www.sigmaaldrich.com (accessed on May 4, 2018).

(27) Skey, J.; O'Reilly, R. K. Facile One Pot Synthesis of a Range of Reversible Addition–Fragmentation Chain Transfer (RAFT) Agents. *Chem. Commun.* **2008**, *31*, 4183.

(28) Perrier, S. 50th Anniversary Perspective: RAFT Polymerization-a User Guide. *Macromolecules* **2017**, *50*, 7433.

(29) Haladjova, E.; Mountrichas, G.; Pispas, S.; Rangelov, S. Poly(Vinyl Benzyl Trimethylammonium Chloride) Homo and Block Copolymers Complexation with DNA. *J. Phys. Chem. B* **2016**, *120*, 2586.

(30) Tsai, T.-H.; Ertem, S. P.; Maes, A. M.; Seifert, S.; Herring, A. M.; Coughlin, E. B. Thermally Cross-Linked Anion Exchange Membranes From Solvent Processable Isoprene Containing Ionomers. *Macromolecules* **2015**, *48*, 655.

(31) Nguyen, T. H.; Kim, S.-H.; Decker, C. G.; Wong, D. Y.; Loo, J. A.; Maynard, H. D. A Heparin-Mimicking Polymer Conjugate Stabilizes Basic Fibroblast Growth Factor. *Nat. Chem.* **2013**, *5*, 221.

(32) Chang, W. B.; Evans, C. M.; Popere, B. C.; Russ, B. M.; Liu, J.; Newman, J.; Segalman, R. A. Harvesting Waste Heat in Unipolar Ion Conducting Polymers. *ACS Macro Lett.* **2016**, *5*, 94.

(33) Thomas, D. B.; Convertine, A. J.; Hester, R. D.; Lowe, A. B.; McCormick, C. L. Hydrolytic Susceptibility of Dithioester Chain Transfer Agents and Implications in Aqueous RAFT Polymerizations †. *Macromolecules* **2004**, *37*, 1735.

(34) Chiefari, J.; Chong, Y. K. B.; Ercole, F.; Krstina, J.; Jeffery, J.; Le, T. P. T.; Mayadunne, R. T. A.; Meijs, G. F.; Moad, C. L.; Moad, G. A.; et al. Living Free-Radical Polymerization by Reversible Addition−Fragmentation Chain Transfer: the RAFT Process. *Macromolecules* **1998**, *31*, 5559.

(35) Mitsukami, Y.; Donovan, M. S.; Lowe, A. B.; McCormick, C. L. Water-Soluble Polymers. 81. Direct Synthesis of Hydrophilic Styrenic-Based Homopolymers and Block Copolymers in Aqueous Solution via RAFT. *Macromolecules* **2001**, *34*, 2248.

(36) Sumerlin, B. S.; Lowe, A. B.; Stroud, P. A.; Zhang, P.; Urban, M. W.; McCormick, C. L. Modification of Gold Surfaces with Water-Soluble (Co)Polymers Prepared via Aqueous Reversible Addition−Fragmentation Chain Transfer (RAFT) Polymerization. *Langmuir* **2003**, *19*, 5559.

(37) Peng, Z.; Wang, D.; Liu, X.; Tong, Z. RAFT Synthesis of a Water-Soluble Triblock Copolymer of Poly(Styrenesulfonate)-B-Poly(Ethylene Glycol)-B-Poly(Styrenesulfonate) Using a Macromolecular Chain Transfer Agent in Aqueous Solution. *J. Polym. Sci. A Polym. Chem.* **2007**, *45*, 3698.

(38) Yokoyama, Y.; Yusa, S.-I. Water-Soluble Complexes Formed From Hydrogen Bonding Interactions Between a Poly(Ethylene Glycol)-Containing Triblock Copolymer and Poly(Methacrylic Acid). *Polym. J.* **2013**, *45*, 985.

(39) Lewis, R. W.; Evans, R. A.; Malic, N.; Saito, K.; Cameron, N. R. Cleavage of Macromolecular RAFT Chain Transfer Agents by Sodium Azide During Characterization by Aqueous GPC. *Polym. Chem.* **2017**, *8*, 3702.

(40) Hiemenz, P. C.; Lodge, T. P. *Polymer Chemistry*, 2nd ed.; CRC Press: Taylor & Francis Group, LLC, 2006.

(41) Kelley, E. G.; Murphy, R. P.; Seppala, J. E.; Smart, T. P.; Hann, S. D.; Sullivan, M. O.; Epps, T. H. Size Evolution of Highly Amphiphilic Macromolecular Solution Assemblies via a Distinct Bimodal Pathway. *Nat. Commun.* **2014**, *5*, 3599.

(42) Cui, H.; Chen, Z.; Zhong, S.; Wooley, K. L.; Pochan, D. J. Block Copolymer Assembly via Kinetic Control. *Science* **2007**, *317*, 647.

(43) Meli, L.; Santiago, J. M.; Lodge, T. P. Path-Dependent Morphology and Relaxation Kinetics of Highly Amphiphilic Diblock Copolymer Micelles in Ionic Liquids. *Macromolecules* **2010**, *43*, 2018.

(44) Wang, Q.; Schlenoff, J. B. The Polyelectrolyte Complex/Coacervate Continuum. *Macromolecules* **2014**, *47*, 3108–3116.

(45) Fu, J.; Fares, H. M.; Schlenoff, J. B. Ion-Pairing Strength in Polyelectrolyte Complexes. *Macromolecules* **2017**, *50*, 1066–1074.

(46) Fares, H. M.; Schlenoff, J. B. Diffusion of Sites Versus Polymers in Polyelectrolyte Complexes and Multilayers. *J. Am. Chem. Soc.* **2017**, *139*, 14656–14667.

(47) Li, L.; Srivastava, S.; Andreev, M.; Marciel, A. B.; de Pablo, J. J.; Tirrell, M. V. Phase Behavior and Salt Partitioning in Polyelectrolyte Complex Coacervates. *Macromolecules* **2018**, *Article ASAP*. DOI: 10.1021/acs.macromol.8b00238

(48) Krogstad, D. V.; Lynd, N. A.; Choi, S.-H.; Spruell, J. M.; Hawker, C. J.; Kramer, E. J.; Tirrell, M. V. Effects of Polymer and Salt Concentration on the Structure and Properties of Triblock Copolymer Coacervate Hydrogels. *Macromolecules* **2013**, *46*, 1512–1518.

(49) Srivastava, S.; Andreev, M.; Levi, A. E.; Goldfeld, D. J.; Mao, J.; Heller, W. T.; Prabhu, V. M.; de Pablo, J. J.; Tirrell, M. V. Gel Phase Formation in Dilute Triblock Copolyelectrolyte Complexes. *Nat. Commun.* **2017**, *8*, 14131.

(50) Jakeš, J. Regularized Positive Exponential Sum (REPES) Program - a Way of Inverting Laplace Transform Data Obtained by Dy-

namic Light Scattering. *Collect. Czech. Chem. Commun.* **1995**, *60*, 1781–1797.

(51) Hammouda, B. "SANS from Polymers—Review of the Recent Literature" *Polym. Rev.* **2010**, *50*, 14.

(52) Lund, R.; Willner, L.; Monkenbusch, M.; Panine, P.; Narayanan, T.; Colmenero, J.; Richter, D. Structural Observation and Kinetic Pathway in the Formation of Polymeric Micelles. *Phys. Rev. Lett.* **2009**, *102*, 188301–188304.

(53) Laaser, J. E.; Jiang, Y.; Petersen, S. R.; Reineke, T. M.; Lodge, T. P. Interpolyelectrolyte Complexes of Polycationic Micelles and Linear Polyanions: Structural Stability and Temporal Evolution. *J. Phys. Chem. B* **2015**, *119*, 15919–15928.

(54) Laaser, J. E.; Lohmann, E.; Jiang, Y.; Reineke, T. M.; Lodge, T. P. Architecture-Dependent Stabilization of Polyelectrolyte Complexes Between Polyanions and Cationic Triblock Terpolymer Micelles. *Macromolecules* **2016**, *49*, 6644–6654.

(55) Jiang, Y.; Sprouse, D.; Laaser, J. E.; Dhande, Y.; Reineke, T. M.; Lodge, T. P. Complexation of Linear DNA and Poly(Styrenesulfonate) with Cationic Copolymer Micelles: Effect of Polyanion Flexibility. *J. Phys. Chem. B* **2017**, *121*, 6708–6720.

Synthesis and Assembly of Designer Styrenic Diblock Polyelectrolytes

Jeffrey M. Ting,[†,‡] Hao Wu,[†] Abraham Herzog-Arbeitman, [§] Samanvaya Srivastava,[⊥] and Matthew V. Tirrell[*,†,‡]

† Institute for Molecular Engineering, University of Chicago, Chicago, Illinois 60637, United States. ‡ Argonne National Laboratory, Lemont, Illinois 60439, United States. § Department of Chemistry, University of Chicago, Chicago, Illinois 60637, United States. ⊥ Department of Chemical and Biomolecular Engineering, University of California, Los Angeles, Los Angeles, California 90095, United States.

[*]Corresponding Email: mtirrell@uchicago.edu

TOC Graphic